




## Case Study

# Visualization of 3D cable between utility poles obtained from laser scanning point clouds: a case study

Masaaki Inoue<sup>1</sup>  · Hitoshi Niigaki<sup>2</sup> · Tomoya Shimizu<sup>1</sup> · Nazuki Honda<sup>1</sup> · Hiroyuki Oshida<sup>1</sup> · Takashi Ebine<sup>1</sup>

Received: 6 May 2021 / Accepted: 26 October 2021

Published online: 08 November 2021

© The Author(s) 2021 [OPEN](#)

## Abstract

We can automate inspection work of infrastructure facilities by analyzing the characteristics of 3D structure information obtained through 3D structure visualization using a point cloud. The safety level of equipment can then be diagnosed quantitatively. In this paper, we investigate the modeling of wire structures such as overhead communication cables between utility poles, which are close to the ground, have many obstructions, and have a complex structure. We evaluate the accuracy of cable models and compare them to the correct model. We use three modeling methods: a machine-learning method based on the extruded surface of a point cloud as a feature, a rule-based method involving principal component analysis, and models generated from a combination of these models. In addition, we focus on modeling overhead cables from field data (urban and suburban). Results show the practicability of modeling overhead cables with a cable length of 10–70 m regardless of the area type. We find that the best cable modeling rate with the precision and recall of 80.76% and 83.84%, respectively, can be obtained using the machine-learning method and by specifying the cable reproduction rate to be 2 m.

## Article highlights

- This study is useful in determining the practicality of 3D visualization of communication cables based on a 3D point cloud.
- Precision and recall are presented as indices to determine the practicality of 3D cable modeling.
- This study provides 3D cable modeling for actual field data (in suburban, bridges, and urban areas).

**Keywords** Mobile mapping system · 3D cable modeling · Point cloud · Precision-recall curve

## Abbreviations

|                     |                              |
|---------------------|------------------------------|
| MMS                 | Mobile mapping system        |
| VLS                 | Vehicle-based laser scanning |
| TLS                 | Terrestrial laser scanning   |
| RANSAC              | Random sample consensus      |
| PCA                 | Principal component analysis |
| PR                  | Precision recall             |
| (PPF <sub>c</sub> ) | Point pair features          |

## 1 Introduction

Optical communications, which is now positioned as a social infrastructure, must be stable and low cost to respond to the rapidly increasing volume of communication traffic accompanying the distribution of digital information such as high-definition video and big data. To ensure such a high level of reliability, it is important to

✉ Masaaki Inoue, [masaaki.inoue.mx@hco.ntt.co.jp](mailto:masaaki.inoue.mx@hco.ntt.co.jp) | <sup>1</sup>NTT Access Network Service Systems Laboratories, NTT Corporation, Ibaraki, Japan. <sup>2</sup>NTT Media Intelligence Laboratories, NTT Corporation, Kanagawa, Japan.



SN Applied Sciences

(2021) 3:860

| <https://doi.org/10.1007/s42452-021-04844-6>

SN Applied Sciences  
A **SPRINGER NATURE** journal

inspect facilities that underpin communication services on a daily basis and the more recent the inspection, the higher the degree of reliability. The wired connection section from a customer building to a communication station comprises various optical communication facilities such as utility poles and optical cables. Image analysis is popular as an automatic inspection technique for these facilities. Siddiqui et al. [1] proposed an inspection method for detecting a variety of facilities attached to utility poles from images taken by a camera using machine learning and classifying them with high accuracy. However, image analysis is not suitable for precise and quantitative spatial diagnosis. Quantitative diagnosis becomes possible through the analysis of 3D digital information of infrastructure facilities converted based on point-cloud information. Digital numerical analysis satisfies our requirements for comprehensive and efficiently performing a large number of outdoor inspections.

Lehtola et al. [2] succeeded in 3D visualization of a building through in-door point cloud acquisition using commercial indoor mapping systems.

Methods for acquiring a 3D point cloud include using airborne laser scanning [3, 4], unmanned aerial vehicles [5], vehicle-based laser scanning (VLS) [6, 7], and terrestrial laser scanning (TLS) [2, 8], the use of which differs depending on the area to be measured. These methods involve

emitting lasers and detecting the return light to acquire a point cloud. Therefore, the shorter the distance to the object, the higher the acquisition density of the point cloud. Communication facilities, the focus of this investigation, are installed mainly along roads. Therefore, VLS is a very effective tool for inspection. A technique to convert camera images into a 3D point cloud was proposed [9, 10], but the accuracy of this method is inferior to using a laser point cloud depending on the photographing environment such as backlighting.

Figure 1 shows an inspection and diagnosis process for outdoor communication structures. A mobile mapping system (MMS) utilizes a 3D laser scanner mounted on a vehicle to acquire raw laser data from communication equipment deployed roadside. The acquired data are processed to calculate a 3D laser point cloud of an absolute coordinate system from the position and attitude of the vehicle and laser data. This point cloud is converted into 3D digital models of outdoor communication structures. Thus, an inspector inspects and diagnoses the condition of the structure in a safe area where reference materials necessary for inspection and diagnosis can be easily obtained without going to the site.

Since a laser point cloud is simply a collection of points, two major steps are necessary to use it for infrastructure inspection. First, a structural model of an object is

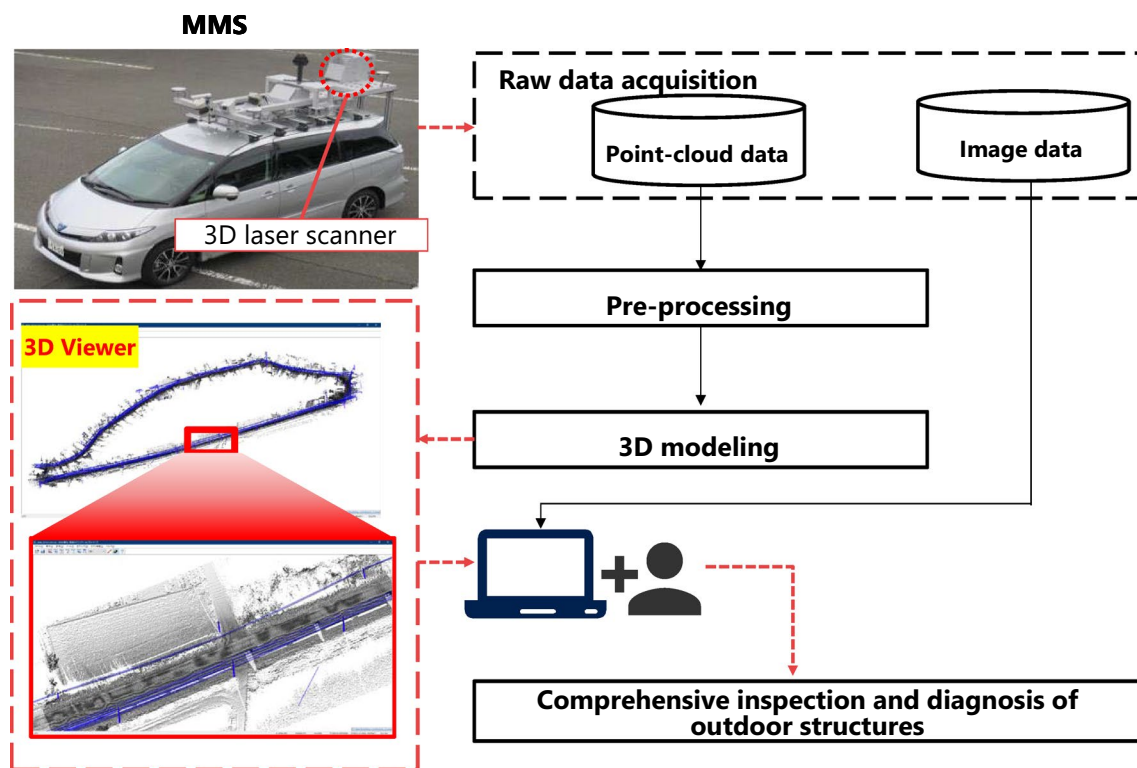


Fig. 1 Inspection and diagnosis process for outdoor communication structures

generated from the laser point cloud. To determine the features of the structure to be measured such as shape and size, it is necessary to extract a point cloud of the feature of the target outdoor structure from the acquired point cloud and recognize it as an individual structure through model generation. The second step is to define and quantify the indicators used for infrastructure inspection based on digital model data. The safety status of the facility to be inspected can be automatically determined based on defined numerical values.

To the best knowledge of the authors, the feasibility of modeling overhead communication cables between utility poles, which are close to the ground, are often surrounded by many obstructions, and have a complex structure, has not yet been thoroughly discussed. In this paper, we carried out modeling of such wire structures to show quantitatively the accuracy of the cable model. Three features of the modeling approach are compared: a machine learning method based on the extruded surface of the point cloud, a rule-based method including principal component analysis, and a model generated from a combination of these models showing optimal parameters. In addition, we focus on modeling overhead cables from field data (urban and suburban) and present quantitative indices that clarify the practicality of 3D visualization.

The rest of the paper is structured as follows. Section 2 outlines 3D modeling techniques. Section 3 compares the 3D modeling results from each technique. Section 4 explains the concept of accuracy evaluation and defines the variables used in the evaluation formula. Section 5 presents verification of the utilized method based on the results of the accuracy evaluation. Finally, Sect. 6 concludes the paper and notes future issues.

## 2 Background

### 2.1 Utility-pole inspection

A 3D-model-generation and inspection-indexing method for utility poles, which are communication facilities, was proposed [11]. This method is used to generate a 3D model as a columnar structure in which utility poles comprise circular models connected in series and the curvature value of the central axis connecting the centers of the circular models is defined as an inspection index. If the safety level of a utility pole decreases due to factors such as cracks, the curvature of the central axis increases. This concept changed inspection using the conventional visual qualitative inspection method to that using a quantitative inspection method. By using the MMS, a laser point cloud of a utility pole that is installed along the road can be acquired while driving

the measurement car, and the inspection work efficiency is greatly improved. A circular model is generated using the Random Sample Consensus (RANSAC) method [12–14], which is robust against noise. For inspection in an area where a vehicle cannot enter, the inspection area can be covered using TLS. It is important to verify the condition of utility poles using these technologies and processes and to open the way for infrastructure inspection by expanding the range of objects for modeling. Expanding the types of modeling objects is an important element for unifying field inspection using 3D digital data. When inspecting communication facilities as a complex network deployed in a planar manner, not only utility poles that exist as columnar structures but also communication cables as wire structures must be included as inspection objects. By managing communication cables as digital data, it is possible to quantify the safety status. For example, in the case of ground height, after modeling a cable, the height information can be used to check if the standard safe height has been met. An example of this is given later in this paper.

### 2.2 3D Cable modeling methods

A utility pole, which has a characteristic columnar structure, has a diameter of approximately 40 cm or less, so it can be easily modeled. On the other hand, since a communication cable laid between utility poles has a small diameter of approximately 4 cm or less, it is difficult to model this wiring structure because the amount of point cloud data is insufficient using the MMS. Some experimental results [15–17] have been reported on 3D wire modeling for power lines between pylons, which exist at several tens of meters high. Point cloud extraction of power lines can be classified from several elements based on geometric assumptions from the processed data set [15] or using a machine learning approach [16]. The point cloud identified as a power line can be reconstructed as a 3D model using the RANSAC algorithm [17]. A point cloud analyzed using these results can be clearly captured because it focuses on the height with little effect from obscured elements. Meanwhile, evaluation of field data of communication cables between utility poles has not been reported. In an area of several meters in height containing many elements such as houses, trees, and signs, it is very difficult to model point groups of communication cables or power lines between utility poles because these elements are partially obscured. Therefore, in this study, we show the feasibility and optimum parameters for evaluation and 3D modeling of a communication cable between utility poles employing a rule-based method using principal component analysis

(PCA) [18] and a machine-learning method using various structural classification approaches [19, 20].

### 2.2.1 Rule-based method

The rule-based method generates segments from a block of points on a communication cable and connects segments of the same shape in time order. The point-cloud data to be analyzed are read and a point cloud within a predetermined range is extracted. Take for example a scenario in which there is a 3D space located between two utility poles and a 3D model of the detected columnar structure is generated. The height of the poles is known in advance as the installation position of the communication line. The 3D model is generated by clustering point clouds

located in a 3D space within a specified range, calculating a direction vector from the clustered point cloud using PCA, detecting the direction vector of the cable structure, and connecting the detected direction vectors, as shown in Fig. 2. A 3D model of the cable structure is generated by connecting the center coordinates of the detected direction vectors.

### 2.2.2 Machine-learning method

The machine-learning method extracts features such as shape and size from a cluster point cloud [19] and models a communication overhead cable.

First, point clouds are clustered based on the similarity of the cross-section of a structure. Based on the results, elongated structures are grouped as identical point-cloud clusters. The feature quantities of the point-cloud cluster within radius  $r$  based on point pair features (PPFs) [21] are extracted using normal and extrusion directions, and the clustered point clouds are classified in terms of whether or not the cable is based on AdaBoost classifiers (Fig. 3). Next, a quadratic curve model is fitted using RANSAC for the point cloud identified as the cable. Finally, whether or not the quadratic curves are connected is determined based on machine learning to generate cable models. The distance between the end points, tangent direction at the end position, and number of errors when two curves are approximated as one curve are used as feature quantities. To generate a database of feature quantities, a measured point cloud and a correct 3D model created on the basis of the point cloud are prepared as data for learning, and the machine-learned results (parameters of the AdaBoost

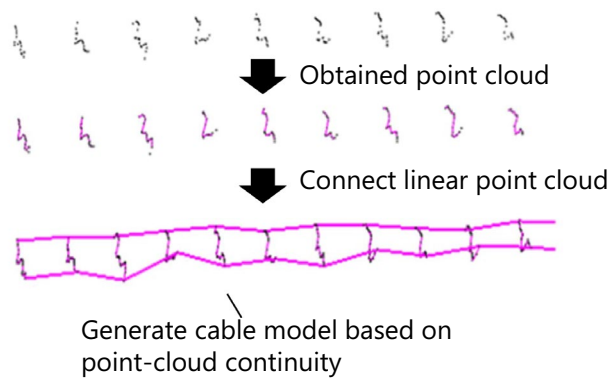


Fig. 2 3D modeling using rule-based method. Generate model by connecting the same direction vectors from PCA results of clustered point cloud

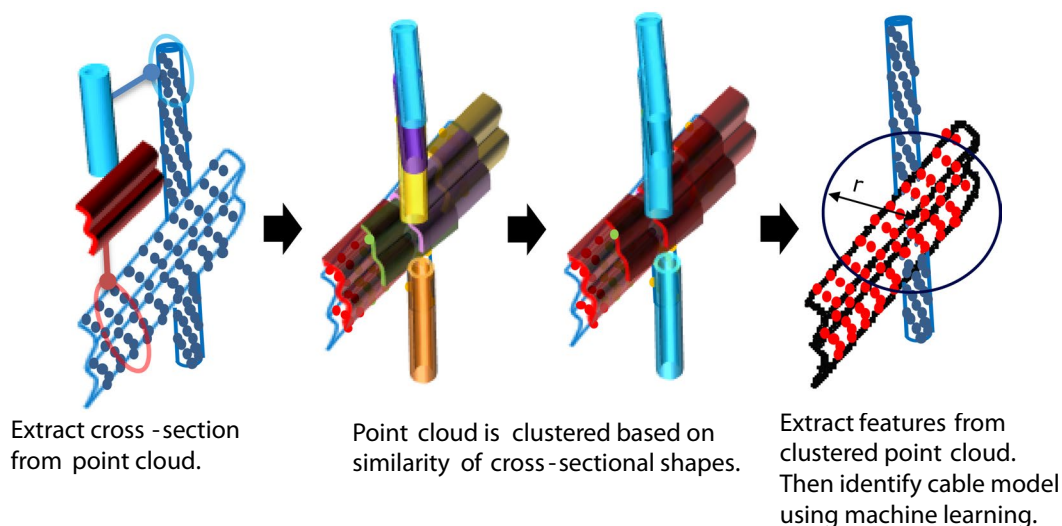


Fig. 3 3D point clustering using machine learning. Feature amount based on PPFs is extracted using normal direction and extrusion direction



discriminator) are stored in advance. Therefore, the modeling accuracy improves by increasing the number of cable-structure models stored in the database, and the results are learned based on the correct 3D model, which approximates the shape of an actual cable structure.

Cable models are not always generated for the same location using the two methods. Some cable models have only machine-learning models and others have only rule-based models. Combining these two models further improves the modeling accuracy. When generated at the same location, either cable model is automatically selected. When laser measurement is carried out using the MMS, the point density to be acquired is different even for objects of equal length due to the distance from the MMS and the presence of occlusions. The method for calculating the degree of inclusion of a point cloud is shown in Fig. 4. A 3D model of a cable structure comprises cable-model-construction points continuously positioned at equal intervals in a 3D space. We calculate a construction point in a point cloud and a construction point not in a point cloud within an arbitrary radius centered on each construction point. Then we calculate the ratio of the construction points within the range including the point cloud among all the construction points as the degree of inclusion of the point cloud. For example, if a cable model is 10 m, and 6 m of it includes a point cloud, the degree of which the cable model includes a point cloud is 60%. The higher the degree of inclusion, the more likely the model is to have the same shape as the actual cable. We calculate the degree of inclusion of a point cloud using the models generated by the rule-base method and the models generated by the machine-learning method. The two models are combined by comparing the inclusiveness of the point clouds in models generated at the same location and selecting models with higher values.

In this study, we focus on evaluating the modeling accuracy of three methods, *i.e.*, machine learning method, rule base method, and combination of both, and the 3D point cloud used is field data. Goto et al. [19] reported that the

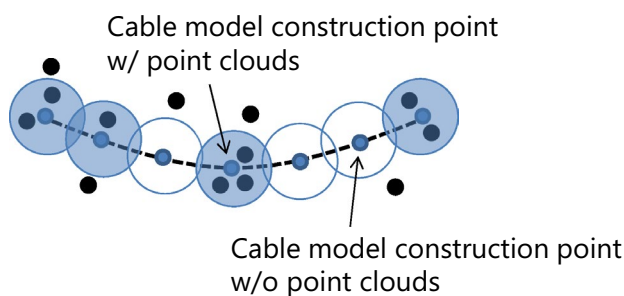


**Fig. 4** Cable-model-construction point used to determine degree of inclusion of point clouds. A model with many cable-model-construction points including a point cloud is similar to an actual cable

model accuracy of the cable installed between utility poles was approximately 21%. The reported results represent a very primitive evaluation method using some verification data. On the other hand, we compare the manually generated accurate data with the mechanically generated cable model to express the modeling accuracy in terms of precision and recall. The field data are obtained from the three areas in which the MMS can move: suburban, bridges, and urban areas. Then, the practical results encourage us to discuss the application of the parameters obtained from the modeling to the inspection.

### 3 Case description

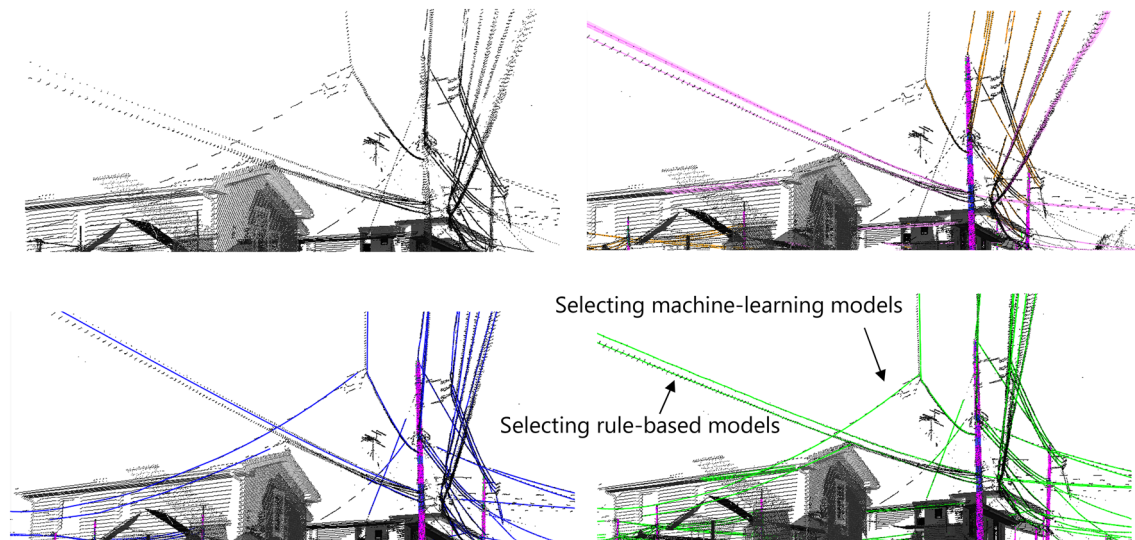
Figure 5 (top left) shows a point cloud including a cable structure straddling utility poles. The point cloud was acquired from an MMS (MMS-Xv220, Mitsubishi Electric, Tokyo, 2016) equipped with a laser (ZF -9012), in which the light emitted from the laser rotated obliquely at 1 million points per second at 1 revolution per 0.01 s. The MMS traveled at a speed of 20–60 km/h in the left lane of a road, and measured the objects along the road including cables on the left and right. It is possible to distinguish between communication lines and power lines based on their height above the ground. The acquired 3D point cloud is output as absolute coordinates and modeled by in-house software based on the method described in Sect. 2.

Figure 5 (top right) shows a 3D wire model of a cable structure created using the rule-based method. The utility poles are pre-modeled using the method described by Matsuda et al. [11]. The clustering range after reading the point cloud is set at 3 cm. A linear element is created from a clustered point cloud and connected to generate the cable model. To reduce the generation of non-cable models, the following two conditions are set.

- A cable model is generated from a 10-m section on the left side and 12-m section on the right side with the lane running from front to back in the figure. In this case study, the point cloud of the cable on the left and right sides is acquired when the vehicle travels on one side of the road. The value for the right section is greater than that on the left because the traffic rules stipulate vehicles drive on the left side of the road.

- The minimum length is set at 5 m for the cable model parallel to the road and at 1 m for the cable model crossing the road. The relationship between the minimum distance setting and the accuracy is described in detail in Sect. 5.1.

In contrast, Fig. 5 (bottom left) shows cable models generated from the machine-learning method. These models are generated using a database containing information regarding cable structures in another part of the same urban area. Point clouds of the communication



**Fig. 5** (Top left) Original point cloud, (top right) 3D rule-based cable models in yellow and pink, (bottom left) 3D machine-learning cable models in blue, and (bottom right) cable model generated from combining both models in green

and electric power cables structures installed roadside at approximately 1 km were recorded and a manually constructed cable model was registered in the database. The model-generation process required approximately 1.5 h on a PC with a Core i9-7900 X CPU and 32 GB of memory. Figure 5 (bottom right) shows a cable model generated by combining the machine-learning and rule-based generation models. There is a rule-based false-generation model on the roof in this model. When models are generated at the same position from both machine-learning and rule-based methods, the one with the highest degree of point-cloud inclusion is selected. These modeling accuracies are evaluated as described in the next section.

## 4 Precision and recall

We evaluate the modeling accuracy of the methods. The indices for modeling accuracy are precision and recall expressed in Eqs. (1) and (2), respectively. Here,  $N_{mg}$  is the number of manually generated correct cable models;  $N_g$  is the number of cable models generated from the machine-learning method, rule-based method, or combination of the two models; and  $M_g$  is the number of matches between  $N_{mg}$  and  $N_g$ .

$$Precision[\%] = M_g / N_g \times 100 \quad (1)$$

$$Recall[\%] = M_g / N_{mg} \times 100 \quad (2)$$

Figure 6 shows a flow chart for evaluating the accuracy of 3D cable modeling. By incorporating the point cloud

into the development tool for 3D modeling with the two methods or the combination of the two, the cable models can be placed and visually recognized in the 3D space. Increasing the amount of learning data is an important factor for improving model accuracy in machine learning. The considered training data used in this study is approximately 1 km of road measured using an MMS. The cables between utility poles are separated and counted. Cables are installed on both sides of the road, and the training data amount is approximately 1000 cables. The models generated from the two methods and the combination of them are compared to the correct model to evaluate modeling accuracy. The correct cable model for comparison is used to identify visually the cable from point-cloud data displayed on a 3D space and to model manually a correct cable structure (sometimes we use image data to distinguish them). In this case study, the generated-cable model is considered correct if it matches more than half the length of the correct-cable model.

## 5 Results and discussion

### 5.1 Precision-recall plots of three methods

The following is from the precision–recall (PR) curve. If precision is high and recall is low, many cable models match the correct cable models, but many correct models are often missing. When recall is high and precision is low however, many correct cable models are generated, but there are also many non-cable models. The aim is to achieve high precision and high recall.

**Fig. 6** Evaluation procedure of 3D cable modeling accuracy

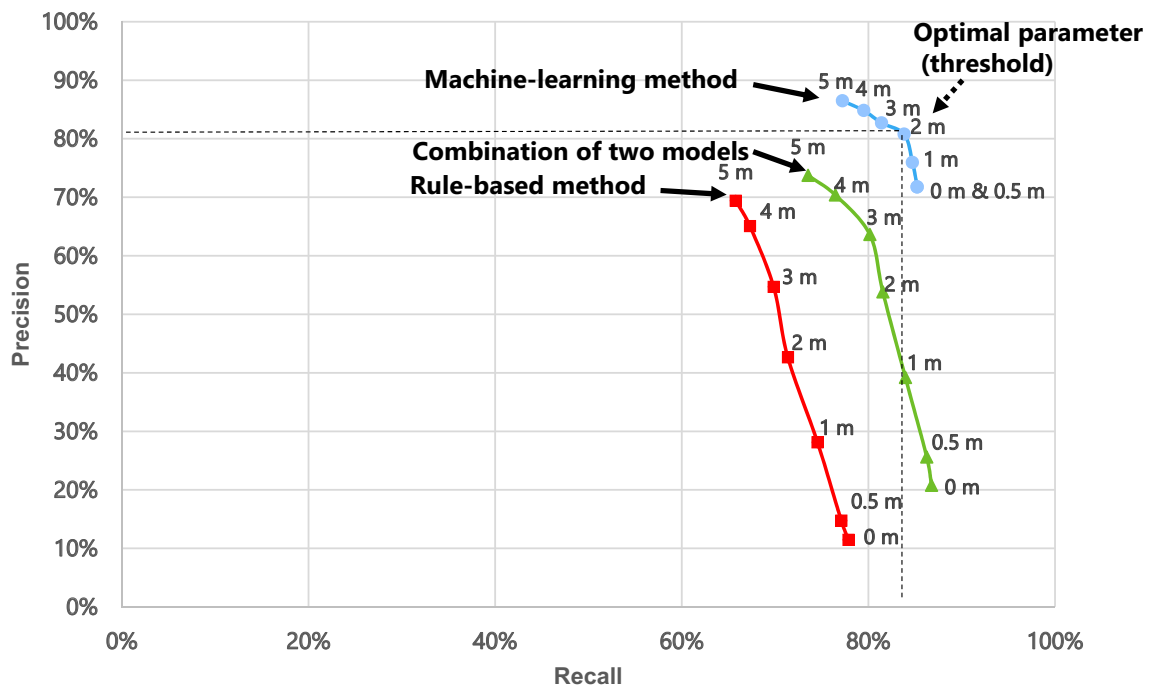
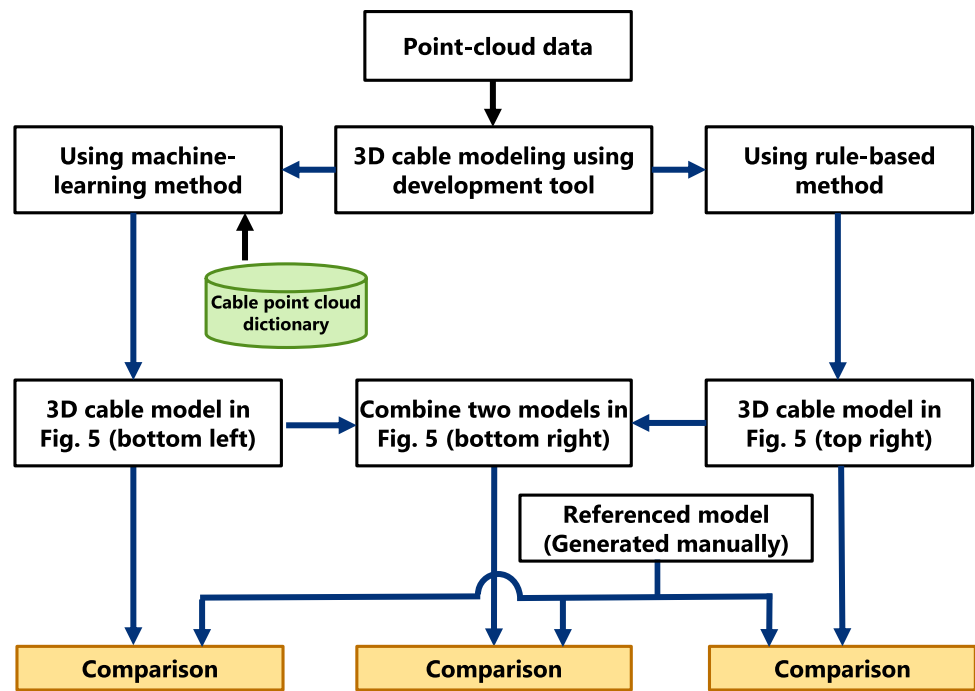


**Fig. 7** PR curves. Precision level for 0 and 0.5 m with machine learning is the same

Figure 7 shows a PR curve modeled from the three types of models. We use the cable-model length as the threshold and plot the results for thresholds of 0 m or longer, 0.5 m or longer, 1 m or longer, 2 m or longer, 3 m or longer, 4 m or longer, and 5 m or longer. The three types of models

show high recall for low thresholds and high precision for high thresholds. This means that for all thresholds, false-generation models, for example, those found in gutters, trees, walls, and road surfaces, are included; however, the lower the threshold (short in length), the more non-cable

models are included. The results of the rule-based method with low thresholds and low precision indicate that short-cable models include many false-generation models. The machine-learning method however exceeds 70% precision even with the cable model with a low threshold of 0 m. Of course, the machine-learning method is not a fully upward-compatible method, as is the rule-based method. The reason for this is that the recall of the model generated with the combination of the two models with a threshold of 0 m is 1.5% higher than that for the model with the same threshold generated from the machine-learning method. That is, a cable that is not modeled from the machine-learning method can be modeled using the rule-based method. Our objective is to achieve well-balanced and highly accurate modeling, not good recall or precision. Therefore, the results suggest that the model generated from the machine-learning method with a threshold of

2 m or longer is the most realistic model with the highest accuracy and reproducibility.

Table 1 gives  $N_g$ ,  $N_{mg}$ , and  $M_g$  of the models with the threshold of 2 m or longer. There are approximately 1.4 km of cables of different diameters running parallel to or across the road, with 786 cables separated by poles. The  $M_g$  value is the highest for the model generated from the machine-learning method, *i.e.*, 659. Regarding the combination model, cables in a close spatial range are combined regardless of machine learning or rule-based methods, so two adjacent cables become one by coupling, and the number of matches is lower than the number of models generated from the machine-learning method. In addition, a cable from the cable structure on the road and wall of a house is generated using the rule-based method, and the number of erroneously generated cable models increases due to this model combination. As a result, the accuracy of the models generated from the combination of methods falls below that of those generated from the machine-learning method as a whole.

**Table 1** Performance of two methods and the combination of the two

|                           | $M_g$ | $N_g$<br>(Precision (%)) | $N_{mg}$<br>(Recall (%)) |
|---------------------------|-------|--------------------------|--------------------------|
| Machine-learning method   | 659   | 816 ( <b>80.76</b> )     | 786 ( <b>83.84</b> )     |
| Rule-based method         | 561   | 1316 (42.63)             | 786 (71.37)              |
| Combination of two models | 641   | 1191 (53.82)             | 786 (81.55)              |

## 5.2 Viewer image

Figure 8 shows optical images of three areas of an outdoor structure obtained from a camera mounted on the MMS, point-cloud data obtained from a laser measuring instrument, and 3D models (Areas 1, 2, and 3) modeled

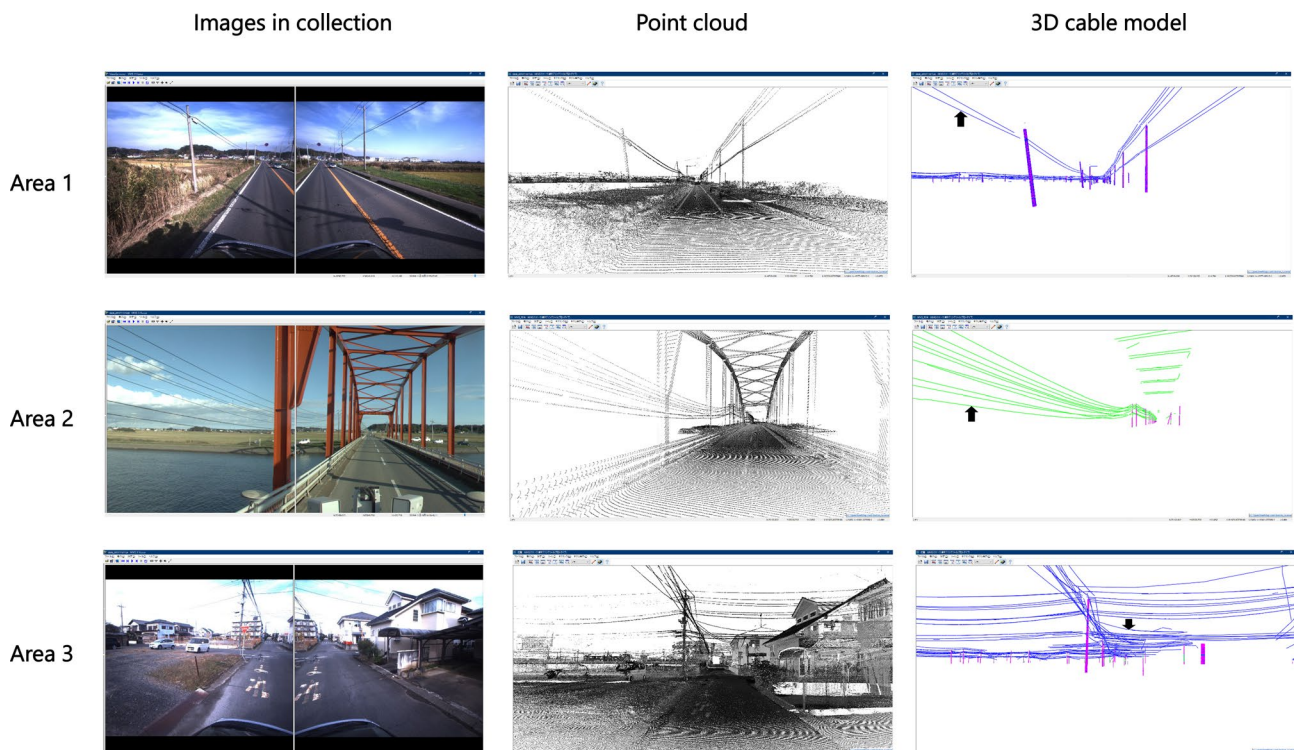


**Fig. 8** Traversed area in captured images, point cloud, and 3D cable model



with the machine-learning method. Area 1 is a suburban area where relatively long cables of 70 m or more are installed and has been accurately modeled. Area 2 is a bridge area and a point cloud of cables parallel to the bridge side is acquired to show cable modeling. Area 3 shows the modeling in which several cables are laid between utility poles in an urban area. These cable models are represented as digital data as given in Table 2. By extracting 3D space information from the digital data of a cable model, the length and slack of the cable, ground height to the road surface, degree of inclusion of the point cloud, and coordinates of the start/end points can be determined. The start/end point information is based on the 9th plane rectangular coordinate system in Japan. In particular, if the ground height is low, it may obstruct

high-altitude vehicles such as aerial vehicles, possibly causing accidents.

Figure 9 shows the display when the user selects the cable model. By selecting a cable model, the ground height between the target cable and ground (yellow line) is displayed, the height of the relevant part can be determined quantitatively, and the safety of the cable can be confirmed. This is achieved using a digitized model.

## 6 Conclusion

We presented the results of a quantitative evaluation of the 3D modeling accuracy of cable models generated from clustered point clouds based on a machine-learning

**Table 2** Summary of configuration data for 3D cable models

|                                        | Long-span cable in suburban area (Area 1)    | Cables laid bridge side (Area 2)             | Cables laid in urban area (Area 3)              |
|----------------------------------------|----------------------------------------------|----------------------------------------------|-------------------------------------------------|
| Cable name                             | Wire_734_653_735_174                         | Wire_00007                                   | Wire_00005                                      |
| Cable length (m)                       | 101.402                                      | 75.015                                       | 11.751                                          |
| Ground height (m)                      | 4.416                                        | 2.331                                        | 4.941                                           |
| Start point information (x, y, z) (m)  | − 8780.59527435, 36,058.6166585, 10.67835901 | 35,166.22950903, 63,719.96301979, 7.93316969 | − 10,469.84601228, 30,750.71856782, 9.02509713  |
| End point information (x, y, z) (m)    | − 8738.47555743, 36,150.704602, 9.92722881   | 35,180.13388047, 63,646.49893655, 9.72085866 | − 10,459.84863012, 30,745.37029633, 11.82488818 |
| Degree of inclusion of point cloud (%) | 100                                          | 99.73                                        | 100                                             |

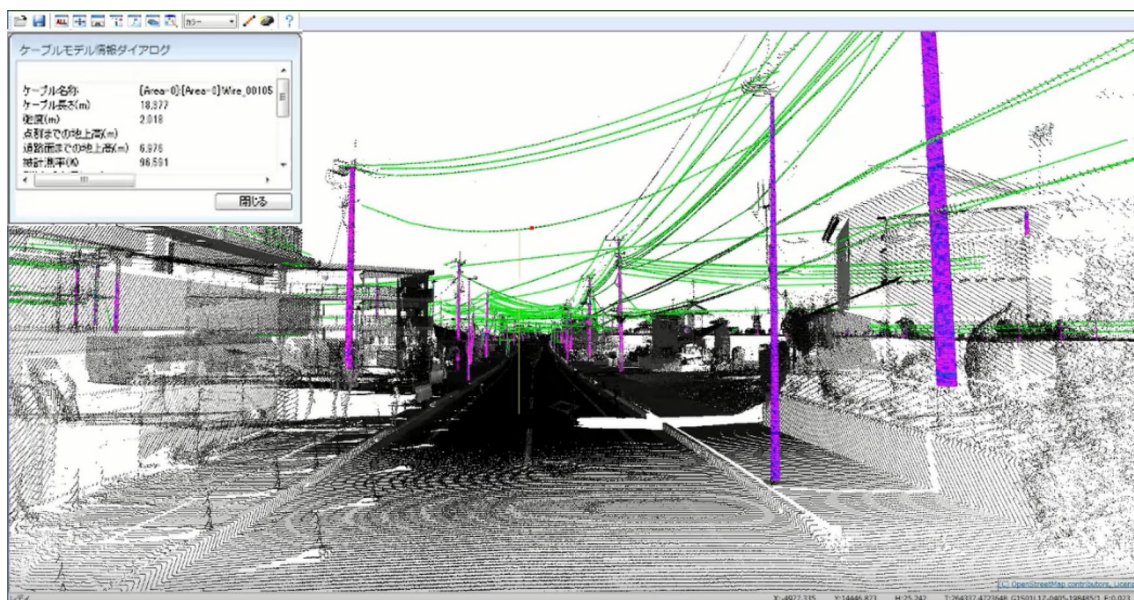


**Fig. 9** Display when user selects cable model

method, rule-based method, and a combination of both, using precision, which indicates the correctness of the model, and recall, which indicates the completeness of the model. The short-cable models included erroneously generated models, and when the threshold was limited to 2 m or longer, the highest recall and precision levels were obtained from that particular model generated from the machine-learning method, *i.e.*, 83.84% and 80.76%, respectively. From the above results, we clarified the accuracy of the cable model between utility poles in detail.

For future work, the focus should be on modeling the section of a cable where the point cloud is missing. An example of an incomplete cable model generated from machine-learning or rule-based methods is a thin cable that connects the main cable to a house. This is because the cable is so thin that it is difficult to train a laser on it and obtain point clouds. Some cables are hidden behind trees. In such cases, a satisfactory point cloud cannot be obtained. Software improvements are needed to allow modeling without obtaining point clouds. Interpolation technology using deep learning such as AI is expected to contribute significantly to such improvements.

**Acknowledgements** We thank NTT advanced technology corporation (NTT-AT) for its efforts in developing the 3D modeling tool. Special thanks are extended to Kenta Yanagisawa, NTT-AT project leader, and Yuji Azuma, NTT-AT project manager, for their guidance on completing the development tool and its usage. We also thank Hiroaki Eizuka for his help with organizing the research data.

**Author contributions** MI obtained the point cloud data shown in the case study, conducted 3D modeling and modeling evaluation, and wrote the first draft of the manuscript. HN devised a machine learning modeling method and edited the manuscript. HO oversaw the entire process of this study. TS, NH, and TE reviewed and revised the first draft. All authors read and approved the final manuscript.

## Declarations

**Conflict of interests** The authors declare that they have no Conflict of interests.

**Data availability** Please contact author for data requests.

**Open Access** This article is licensed under a Creative Commons Attribution 4.0 International License, which permits use, sharing, adaptation, distribution and reproduction in any medium or format, as long as you give appropriate credit to the original author(s) and the source, provide a link to the Creative Commons licence, and indicate if changes were made. The images or other third party material in this article are included in the article's Creative Commons licence, unless indicated otherwise in a credit line to the material. If material is not included in the article's Creative Commons licence and your intended use is not permitted by statutory regulation or exceeds the permitted use, you will need to obtain permission directly from the copyright holder. To view a copy of this licence, visit <http://creativecommons.org/licenses/by/4.0/>.

## References

1. Siddiqui ZA, Park U, Lee S, Jung N, Choi M, Lim C, Seo J (2018) Robust powerline equipment inspection system based on a convolutional neural network. *Sensors* 18(11):3837. <https://doi.org/10.3390/s18113837>
2. Lehtola VV, Kaartinen H, Nuechter A, Kaijaluo R, Kukko A, Litkey P, Honkavaara E, Rosnell T, Vaaja MT, Virtanen J, Kurkela M, Issaoui AE, Zhu L, Jaakkola A, Hyyppä J (2017) Comparison of the selected state-of-the-art 3D indoor scanning and point cloud generation methods. *Remote sensing* 9(8):796. <https://doi.org/10.3390/rs9080796>
3. Dorninger P, Pfeifer N (2008) A comprehensive automated 3D approach for building extraction, reconstruction, and regularization from airborne laser scanning point clouds. *Sensors* 8(11):7232–7343. <https://doi.org/10.3390/s8117323>
4. Mewis P (2021) Estimation of vegetation-induced flow resistance for hydraulic computations using airborne laser scanning data. *Water* 13(13):1864. <https://doi.org/10.3390/w13131864>
5. Ham Y, Han KK, Lin JJ, Golparvar-Fard M (2016) Visual monitoring of civil infrastructure systems via camera-equipped unmanned aerial vehicles (UAVs): A review of related works. *Visualization in Engineering* 4:1
6. Lehtomäki M, Jaakkola A, Hyyppä J, Kukko A, Kaartinen H (2010) Detection of vertical pole-like objects in a road environment using vehicle-based laser scanning data. *Remote Sensing* 2(3):641–664. <https://doi.org/10.3390/rs2030641>
7. Kalenjok S, Lienhart W, Rebhan MJ (2021) Processing of mobile laser scanning data for large-scale deformation monitoring of anchored retaining structures along highways. *Comput Aided Civ Inf* 36:678–694. <https://doi.org/10.1111/mice.12656>
8. Stal C, Verbeurgt J, De Sloover L, Wulf A (2021) Assessment of handheld mobile terrestrial laser scanning for estimating tree parameters. *J For Res* 32:1503–1513. <https://doi.org/10.1007/s11676-020-01214-7>
9. Bae H, Golparvar-Fard M, White J (2013) High-precision vision-based mobile augmented reality system for context-aware architectural, engineering, construction and facility management (AEC/FM) applications. *Visualization in Engineering* 1:3
10. Xia C, Han S, Pan X (2020) Object spatial localization by fusing 3D point clouds and instance segmentation. *SN Appl*. <https://doi.org/10.1007/s42452-020-2210-9>
11. Matsuda S, Goto T, Honda R, Kajiwara Y (2018). Improving telecommunication facility maintenance through better estimation accuracy of pole bend. In proceedings of the 67th international cable and connectivity symposium 2018, (pp. 763–767), Providence, RI.
12. Schnabel R, Wahl R, Klein R (2007) Efficient RANSAC for point-cloud shape detection. *Computer Graphics Forum* 26(2):214–226
13. Holies R, Fischler M. (1981). A RANSAC-based approach to model fitting and its application to finding cylinders in range data. In proceedings of the 7th international joint conference on artificial intelligence, (pp. 637–644), Vancouver, BC.
14. Rusu R, Blodow N, Marton Z, Soos A, Beetz M (2007). Towards 3D object maps for autonomous household robots. In proceedings of the international conference on intelligent robots and systems, (pp. 3191–3198), San Diego, CA.
15. Nardinocchi C, Balsi M, Esposito S (2020) Fully automatic point cloud analysis for powerline corridor mapping. *IEEE Trans Geosci Remote Sens* 58(12):8637–8648. <https://doi.org/10.1109/TGRS.2020.2989470>
16. Pu S, Xie L, Ji M, Zhao Y, Liu W, Wang L, Yang F, Qiu D (2019). Real-time powerline corridor inspection by edge computing of UAV lidar data. In proceedings of the international archives of

- the photogrammetry, remote sensing and spatial information sciences, (pp. 547–551), Enschede.
17. Guo B, Li Q, Huang X, Wang C (2016) An improved method for power-line reconstruction from point cloud data. *Remote Sensing* 8(1):36. <https://doi.org/10.3390/rs8010036>
  18. Goto T, Waki M, Katayama K (2018). Highly accurate and efficient maintenance technology for optical cables and utility poles. In proceedings of the optical fiber communication conference and exposition, (pp. 1–3), San Diego, CA.
  19. Niigaki H., Shimamura J, Kojima A (2015). Segmentation of 3D lidar points using extruded surface of cross section. In proceedings of the 2015 international conference on 3D Vision, (pp. 109–117), Lyon.
  20. Golovinskiy A, Kim VG, Funkhouser T (2009). Shape-based recognition of 3D point clouds in urban environments. In proceedings of the 2009 IEEE 12th international conference on computer vision, (pp. 2154–2161), Kyoto.
  21. Drost B, Ulrich M, Navab N, Ilic S (2010). Model globally, match locally: Efficient and robust 3D object recognition. In proceedings of the 2010 IEEE computer society conference on computer vision and pattern recognition, (pp. 998–1005), San Francisco, CA.

**Publisher's Note** Springer Nature remains neutral with regard to jurisdictional claims in published maps and institutional affiliations.